Preprint typeset in JINST style - HYPER VERSION

Addendum to the CAN-037 note on the first results of the SDHCAL technological prototype

CALICE collaboration.

ABSTRACT: In this addendum, a new analysis of the data accumulated during the August-September 2012 campaign of the SDHCAL prototype exposure to pion and electron beams at the SPS-H6 line is presented. The selection of the pion sample differs from that presented in the CAN-037 note. The new selection is based on very simple criteria. Similar resolution to that presented in the CAN-037 note is found at high energy (>30 GeV). At low energy the resolution found with the present selection is about 15% better. This is mostly due to the fact that electron rejection is more efficient in the present selection.

Contents

1. Introduction **1**

2. Hadronic showers selection **1**

2.1 Proton contamination 1

2.2 Electron contamination 2

2.3 Muon and cosmic contamination 3

2.4 Neutral contamination 3

3. Results **4**

4. Conclusion **10**

A. Result summary **11**

B. Energy distributions **12**

C. Shower selection **13**

1. Introduction

The same set of events collected in the August-September 2012 campaign and presented in the CAN-037 note was reanalyzed. As mentioned in the note only runs with less than 1000 particles per spill were studied. This restriction was applied to avoid efficiency loss in the GRPC in case of high particle rate.

2. Hadronic showers selection

2.1 Proton contamination

The H6 pion beam is contaminated by different kinds of particles. Some particle, (eg. protons) interact in the prototype hadronically and the showers they produce are expected to be similar to those of the pions at high energy where the effect of mass difference is negligible. Since the proton contamination is present in pion beams at energies above 20 GeV in the H6 line, as was measured by the ATLAS Collaboration [1], protons will be treated as pions in this addendum even though the proton interaction length is slightly lower than that of the pion. This means that proton induced showers have more hits.

2.2 Electron contamination

Electrons are also present in the pion beam despite the use of a lead filter to reduce their number. The absence of a Cherenkov counter or any other detector able to discriminate electrons against pions makes it necessary to find other means to eliminate the electrons in our hadronic sample. Using topological selections based on the fractal dimensions method associated to the compactness criteria presented in the CAN-037 note is one way. Another way is to use the fact that electrons start their electromagnetic shower in the prototype in the first plates. This is due to the fact that the radiation length in steel is 1.76 cm. For data which feature electromagnetic or hadronic showers, requiring that the shower starts in the fifth layer or after should in principle kill almost all of the electrons since this represents about 6 X_0. To define the start of the shower we look for the first layer with more than 4 fired pads. To eliminate fake shower starts due to accidental noise or local high multiplicity effect, three consecutive layers were required to have more than 4 fired pads as well. Electromagnetic showers in the energy range between 5 and 80 GeV are longitudinally contained in less than 30 layers of our SDHCAL prototype, as shown in Figure 1.

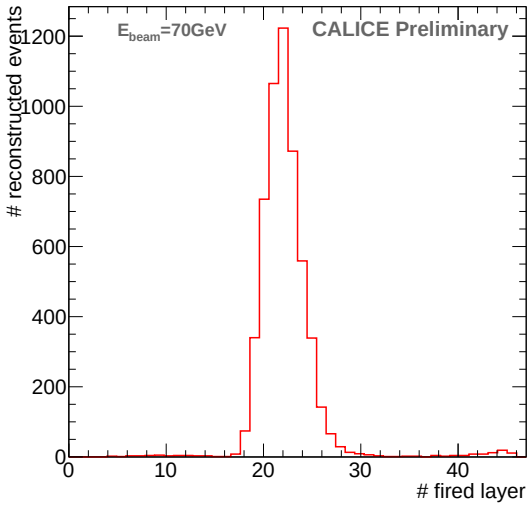

Figure 1. Distribution of number of fired layers for a 70 GeV electron run. The small peak after 40 fired layers is due to remaining pions and muons.

This electron rejection criterion was therefore applied only for events in which no more than 30 layers containing each more than 4 fired pads are found. This limitation helps to minimize the loss of true pion hadronic showers at high energy where the number of fired layers exceeds 30. In this way high energy pions starting their shower in the first layers are not rejected. Low energy pions have relatively smaller number of fired layers and are fully contained in the SDHCAL. For these pions the effect of this selection is only statistical. Pions that start showering in the first 4 layers are lost but no bias on the energy resolution is introduced. To check the rejection power of this selection, it was applied to electron runs at different energies collected during the same campaign. Figure2 shows the distribution of number of hits before and after the selection for 10, 40 and 70 GeV electron runs. It shows clearly the rejection power of this selection.

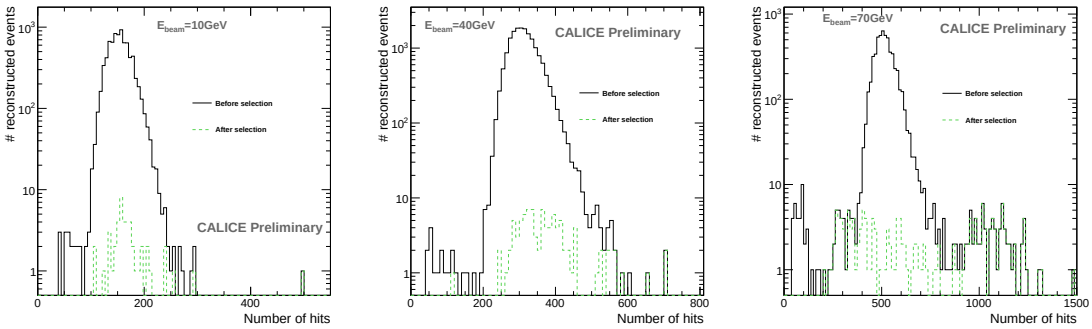

Figure 2. Distribution of number of hits for 10, 40 and 70 GeV electron runs before (solid black line) and after (dashed green line) electron rejection.

2.3 Muon and cosmic contamination

Muons are also present in the pion beam. They are produced by pions stopped in the collimator or those decaying before reaching the prototype. To eliminate these muons as well as the cosmic contamination the average number of hits per fired layer was requested to be greater than 2.2. This is higher than the average pad multiplicity which was found to be 1.73 [2]. This eliminates the non radiative muons. To eliminate the radiative ones, as can be seen in Figure 3, we require that the ratio between the number of layers in which the root mean square of the hits position in the plane (x,y) is exceeding 5 cm in both x and y directions and the total number of layers with at least one fired hit is more than 20%. The effect of this selection on showering pions is limited. Indeed the ratio of 20% corresponds in this case to pions which start showering in the last ten layers of our SDHCAL prototype. This means those surviving after 4.5 λ_I. which is a negligible number of pions.

2.4 Neutral contamination

To eliminate neutral contamination in our selection, events with strictly less than 4 hits in the first 5 layers are not considered. This criterion eliminates most of the cosmics as well. In addition to the previous criteria and in order to avoid the presence of more than one incoming particle in the final sample, events for which the first five layers have hits separated by more than 5 cm are eliminated. The selection criteria are summarised in Table 2.4

Electron rejection	Shower start ≥ 5 or $N_{layer} \geq 30$
Muon rejection	$\frac{N_{hit}}{N_{layer}} > 2.2$
Radiative muon rejection	$\frac{N_{layer \setminus RMS>5cm}}{N_{layer}} > 20\%$
Neutral rejection	$N_{hit \in First\ 5\ layers} \geq 4$

Table 1. Summary of the different cuts applied to select the pions

The result of such selection is shown in Figure 4 for three energies; 10, 30 and 80 GeV where the total number of hits of the collected events is drawn. Figure 10 in Appendix C shows also

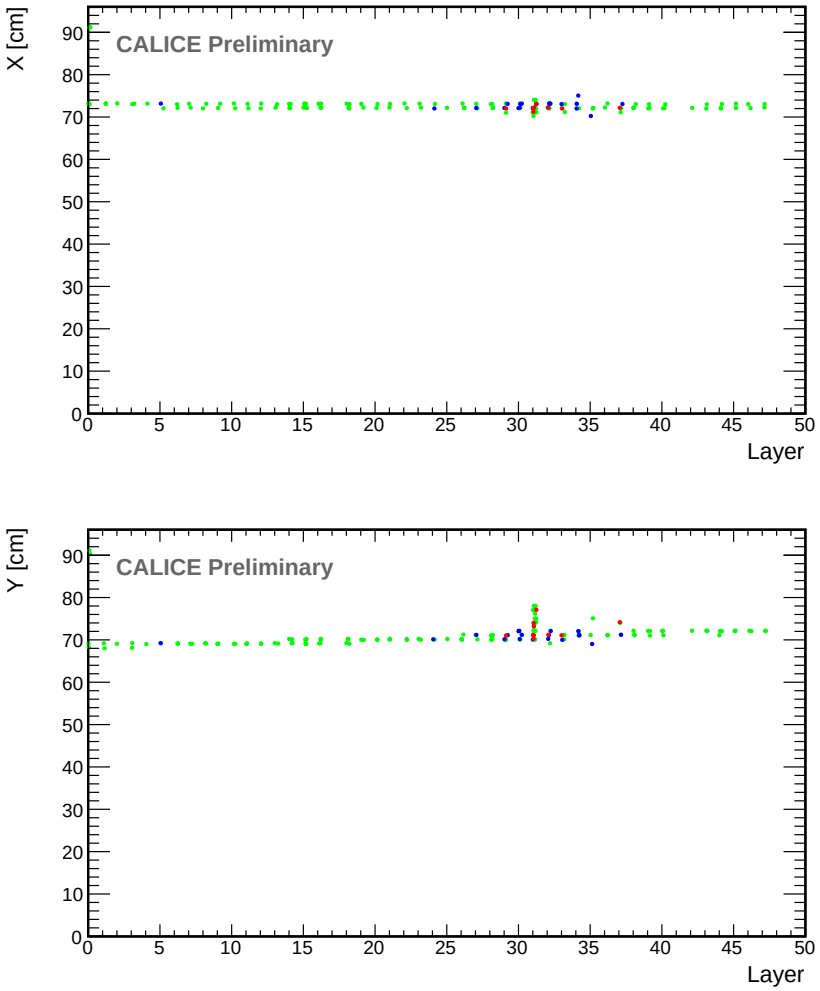

Figure 3. A 50 GeV radiative muon event display with red color indicating the highest threshold fired pads, blue color indicates the middle threshold, and green color is for the lowest one.

result of this selection for other beam energies. Remaining electrons are not important as it can be seen in Figure 2. One can see that at high and intermediate energy the selection does not affect the pion component (right tail). At lower energy, the shape is maintained but there is a loss in the total number of pion events as was mentioned before. In both cases, the fact that the shape of the pion component is not affected ensures that our selection does not bias the hits distribution of pions and hence the energy resolution should not be affected by this selection.

3. Results

After applying the previous selection, the same procedure, done in [2] section 4.2, is used to determine the reconstructed energy of hadronic showers. The shower energy is given by:

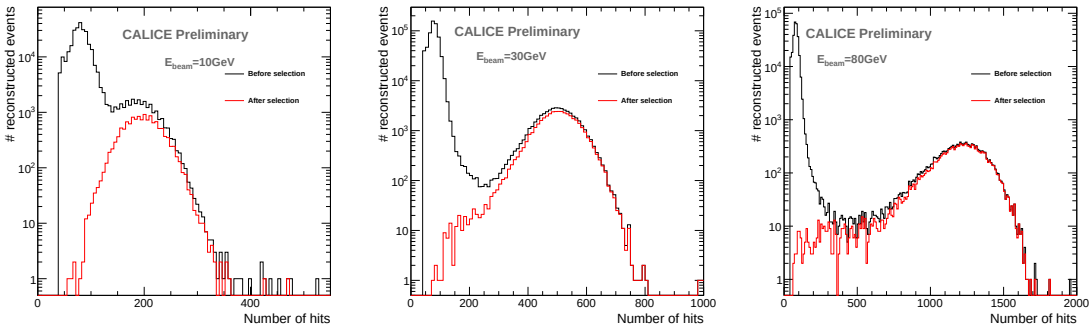

Figure 4. Number of hits for 10, 30 and 80 GeV pion runs before (black line) and after (red line) full selection.

$$E_{reco} = \alpha N_1 + \beta N_2 + \gamma N_3 \tag{3.1}$$

where α, β, γ are quadratic functions of total number of hits and N_i is the number of hits for which the i^{th} threshold has been crossed. These coefficients are extracted from a χ^2 minimisation using few energy points.

$$\chi^2 = \sum_{i=1}^{N} \frac{(E^i_{beam} - E^i_{reco})^2}{E^i_{beam}} \tag{3.2}$$

The evolution of these paramaters is shown in Figure 5.

These coefficients are then used to estimate the energy of incoming particles. Figure 6 shows the energy distributions for 10, 30, 50 and 80 GeV pions. The distributions are fitted with the Crystal Ball function defined in [2] (Appendix A) in order to take into consideration the tail at low energy. A gaussian fit was also performed and used for estimation of systematic uncertainties.

Figure 7 shows the mean reconstructed energy for pion showers versus the beam energy and the relative deviation to the beam energy.

Figure 8 shows the energy resolution as a function of the beam energy defined as $\frac{\sigma}{E_{beam}}$ where σ is the gaussian width given by the Crystal Ball fit. All these results are summarized in the Table A

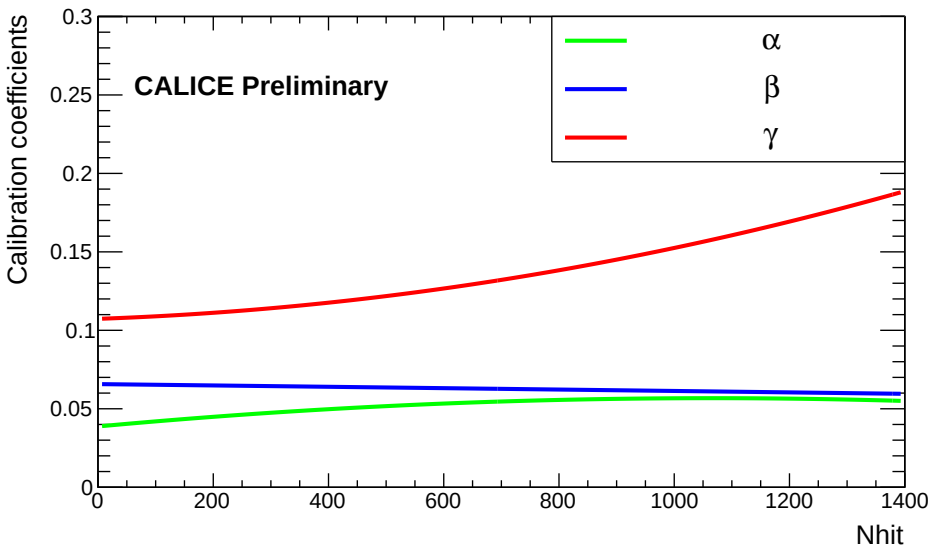

Figure 5. Evolution of the coefficient α (green), β (blue) and γ (red) in terms of the total number of hits.

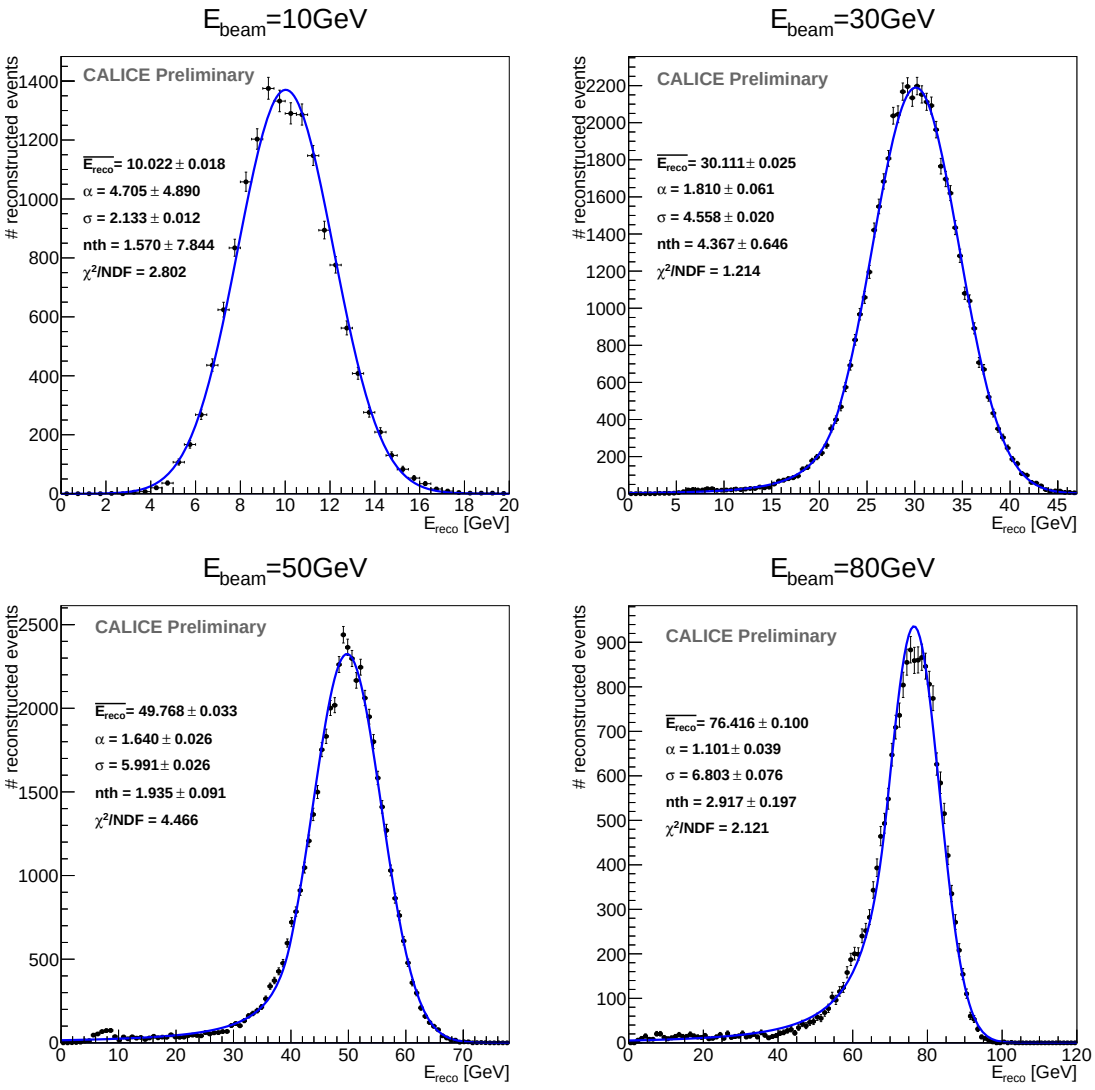

Figure 6. Reconstructed energy for pion showers of 10, 50 GeV (left) and 30, 80 GeV (right) using the threshold informations. The distributions are fitted with a Crystal Ball function.

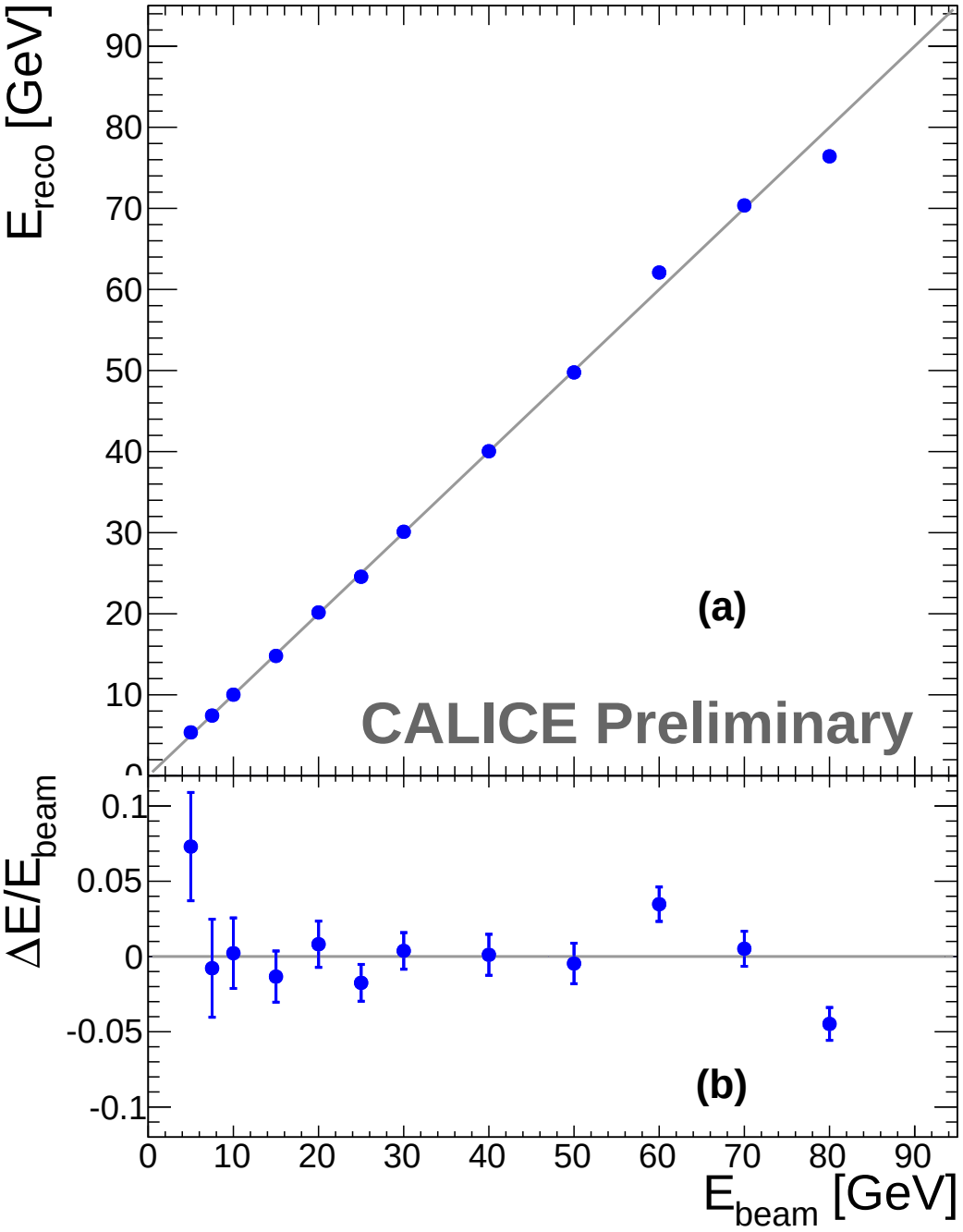

Figure 7. (a): Mean reconstructed energy for pion showers and (b): relative deviation of the pion mean reconstructed energy with respect to the beam energy as a function of the beam energy.The reconstructed energy is computed using the three thresholds information, and the distributions are fitted with a Crystal Ball function.

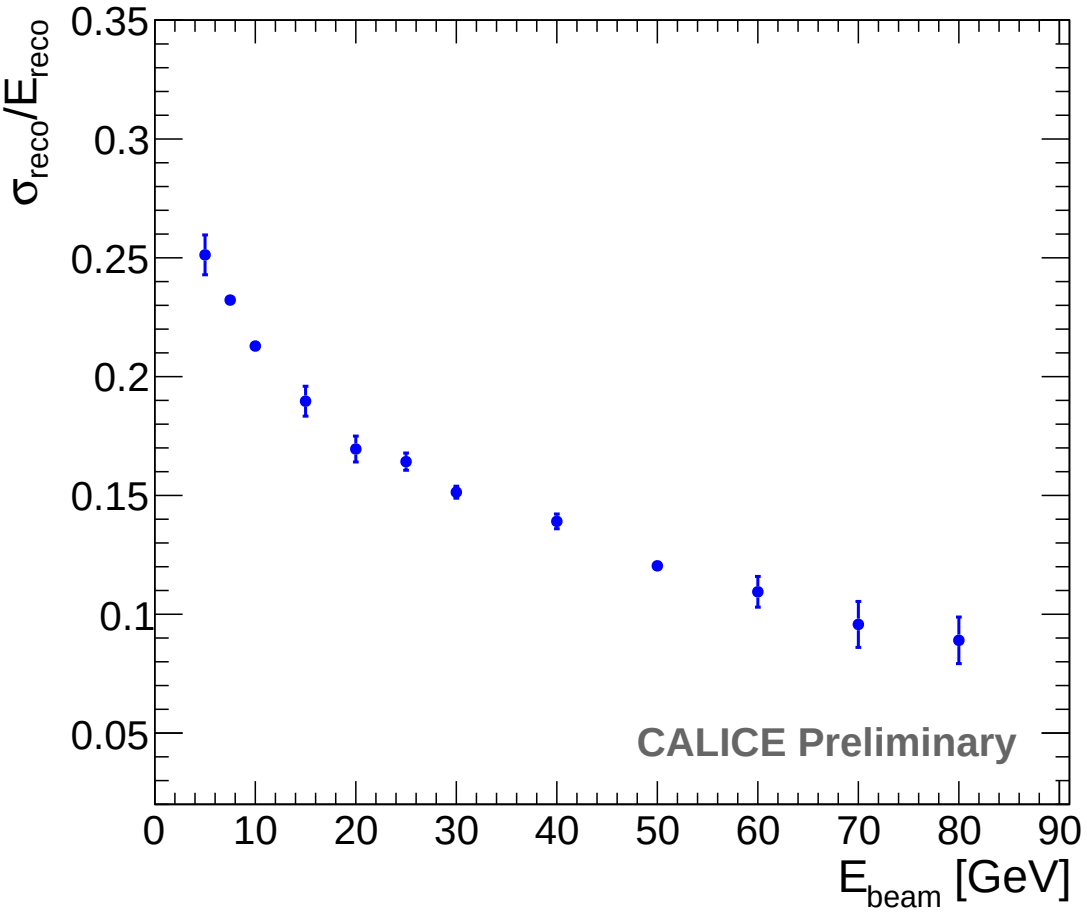

Figure 8. $\frac{\sigma(E)}{E}$ of the reconstructed pion energy E as a function of the beam energy. The reconstructed energy is computed using the three thresholds information, and the distributions are fitted with a Crystal Ball function.

4. Conclusion

The results obtained with this new analysis confirm those presented in the CAN-037 note. The improvement on energy resolution at low energy (< 15 GeV) shows that electron rejection was probably not completely effective in the previous analysis.

References

[1] E. Abat *et al*, *Study of energy response and resolution of the ATLAS barrel calorimeter to hadrons of energies from 20 to 350 GeV*, NIM A, Volume 62, Issues 1-3, 1-21, September 2010.

[2] The CALICE Collaboration, *First results of the CALICE SDHCAL technological prototype*, CALICE Analysis Note CAN-037, 30.11.2012

A. Result summary

$E_{beam}(GeV)$	$E_{reco}(GeV)$	$\frac{\Delta E}{E_{beam}}(\%)$	$\frac{\sigma E_{reco}}{E_{reco}}(\%)$
5	5.365 ± 0.14	7.3 ± 3.6	25.1 ± 0.8
7.5	7.442 ± 0.18	-0.7 ± 3.3	23.2 ± 0.2
10	10.02 ± 0.15	0.2 ± 2.3	21.3 ± 0.2
15	14.80 ± 0.12	-1.3 ± 1.7	18.9 ± 0.6
20	20.16 ± 0.12	0.8 ± 1.5	16.9 ± 0.5
25	24.56 ± 0.08	-1.8 ± 1.2	16.4 ± 0.4
30	30.11 ± 0.09	0.3 ± 1.2	15.1 ± 0.3
40	40.05 ± 0.19	0.1 ± 1.3	13.9 ± 0.3
50	49.77 ± 0.20	-0.5 ± 1.3	12.0 ± 0.1
60	62.09 ± 0.14	3.5 ± 1.1	10.9 ± 0.6
70	70.36 ± 0.17	0.5 ± 1.2	9.6 ± 1.0
80	76.42 ± 0.20	-4.5 ± 1.1	8.9 ± 1.0

Table 2. Mean reconstructed energy E_{reco}, relative deviation to the beam energy $\frac{\Delta E}{E_{beam}}$ and energy resolution $\frac{\sigma E_{reco}}{E_{reco}}$ quoted in %. σE is the gaussian width given by the Crystal Ball fit.

B. Energy distributions

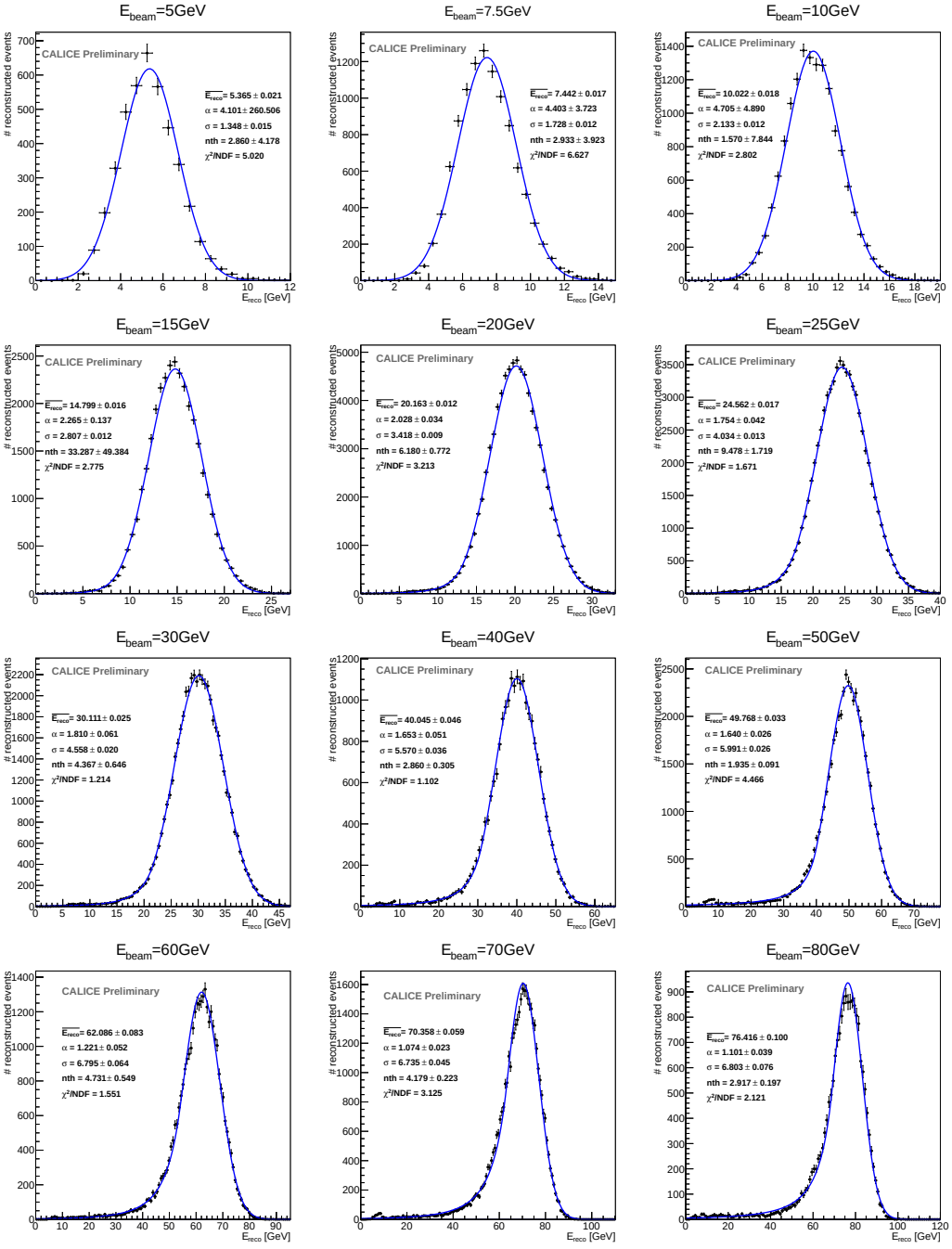

Figure 9. Reconstructed energy for pion showers from 5 (top left) to 80 GeV (bottom right) using the threshold informations. The distributions are fitted with a Crystal Ball function.

C. Shower selection

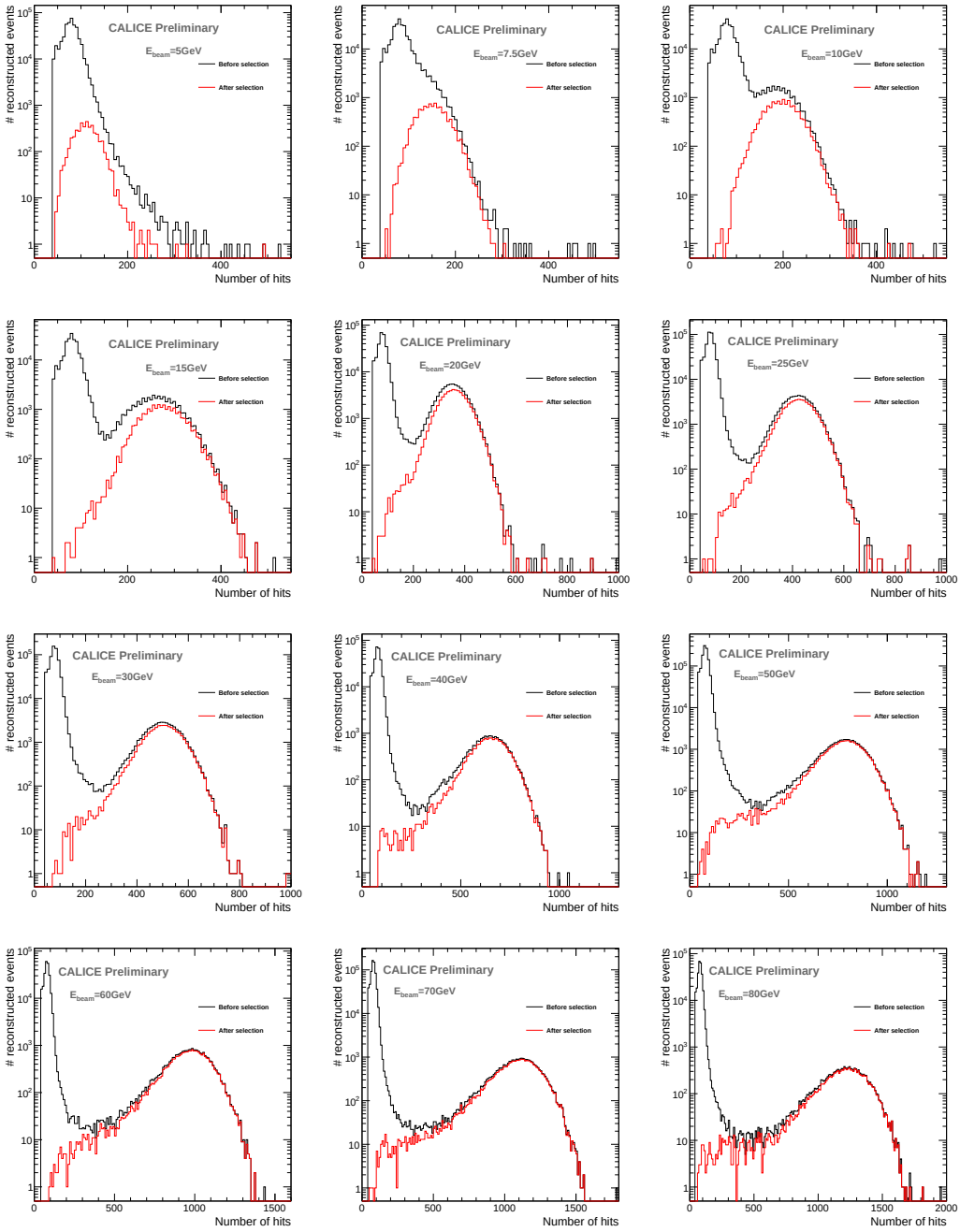

Figure 10. Distribution of number of hits for pion runs from 5 (top left) to 80 GeV (bottom right) before (black line) and after (red line) selections.